Journal of Solid State Chemistry 218 (2014) 64–70

Contents lists available at ScienceDirect

Journal of Solid State Chemistry

journal homepage: www.elsevier.com/locate/jssc

A new carboxyl-copper-organic framework and its excellent selective absorbability for proteins

Linyan Yang [a], Liangliang Xin [b], Wen Gu [a,c], Jinlei Tian [a,c], Shengyun Liao [a], Peiyao Du [a], Yuzhang Tong [a], Yanping Zhang [a], Rui Lv [a], Jingyao Wang [a], Xin Liu [a,c,*]

[a] Department of Chemistry, Nankai University, Tianjin 300071, China
[b] School of Science, Tianjin University, Tianjin 300072, China
[c] Tianjin Key Laboratory of Metal and Molecule Based Material Chemistry, Tianjin 300071, China

ARTICLE INFO

Article history:
Received 5 February 2014
Received in revised form
19 May 2014
Accepted 24 May 2014
Available online 16 June 2014

Keywords:
Carboxyl-copper-organic framework
Luminescent
Protein adsorption
XPS

ABSTRACT

One-pot solvothermal treatments of $CuCl_2 \cdot 2H_2O$, H_2**L** (5-(3-methyl-5-(pyridin-4-yl)-4*H*-1,2,4-triazol-4-yl) isophthalic acid) and $Sm(NO_3)_3 \cdot 6H_2O$ in water yielded a rare carboxyl-copper-organic framework, $[Cu(HL)]_n \cdot nH_2O$ (**1**). The existence of carboxyl groups in compound **1** may be due to the interference of $Sm(NO_3)_3 \cdot 6H_2O$ at the relatively high temperature and autogenous pressure of the reaction. Compound **1** has been characterized by single-crystal X-ray diffraction, PXRD, IR, and elemental analysis. Compound **1** is a 3D coordination polymer, and an xfe-4-Fddd, ($4^2.6.8^3$) topology in **1** is created. In addition, the optical properties have been investigated. Rhodamine B dyeing experiments exhibited that there were residual carboxyl groups on the surface of compound **1**. UV–vis results showed that more lysozyme was adsorbed onto the surface of compound **1** than BSA at pH 7.4. At the same time, XPS spectra were also investigated to verify the results.

1. Introduction

Considerable attention has been paid to the study of transition metal coordination polymers not only because of non-linear optics [1,2], gas absorption [3–5], luminescence [6,33], magnetism [34], medicine [35], and catalytic properties [36,37], but also their fascinating architectures [38,39]. Many chemical functionalities are incompatible with the conditions for MOF assembly, and cannot be obtained covalently attached within MOF cavities via traditional synthetic routes. For example, MOFs with struts containing free carboxylic acids [7] or pyridines [8] remain rare, as these moieties often serve as the key coordinating elements of the MOF frameworks. This can be explained by the tendency of such reactive groups to engage in framework building through coordination or hydrogen bonding. The appeal of MOF materials that have free carboxylic acids is clear: they can be further modified using a wide range of reactions to afford new MOFs with different capabilities [9]. For example, such a MOF could be functionalized with a variety of metals, generating a series of new MOF materials with metal carboxylates in their pores, where each one can be used for a particular catalytic reaction [8,10]. Alternatively, the varying affinities that metal carboxylates have for different chemical species could be exploited to separate specific chemical mixtures [11–13]. In view of free carboxylic acids from the surface of MOF, we have considered the possibility of protein adsorption. In physiological media, most proteins carry a net charge, with the sign and magnitude of the net charge depending on the isoelectric point of the protein (pI). Electrostatic interactions between proteins and charged surfaces, therefore, often play a major role in the adsorption behavior of proteins [14–16]. Herein, we present a novel copper-based MOF $[Cu(HL)]_n \cdot nH_2O$ (**1**; H_2**L**=5-(3-methyl-5-(pyridin-4-yl)-4*H*-1,2,4-triazol-4-yl) isophthalic acid). The ligand H_2**L**, which can be obtained from cheap starting materials by a two-step synthesis in good yield, combines carboxylate, triazole, and pyridine functions and is adopted from a recently presented series of linkers. We investigated the amounts of bovine serum albumin (BSA, negatively charged at pH 7.4) and lysozyme (positively charged at pH 7.4) adsorbed onto negatively MOF to monitor the effect of electrostatic attraction and repulsion on the amount of adsorbed proteins. At the same time, XPS spectra were also investigated to verify the results.

2. Experimental section

2.1. Materials and physical measurements

Lysozyme was purchased from Sigma-Aldrich. Bovine serum albumin (BSA) was obtained from Amresco Inc. (Solon, OH).

* Corresponding author at: Department of Chemistry, Nankai University, Tianjin 300071, China. Tel.: +86 13512865 360; fax: +86 22 2350 2779.
E-mail address: liuxin64@nankai.edu.cn (X. Liu).

http://dx.doi.org/10.1016/j.jssc.2014.05.019
0022-4596/

All commercially available chemicals and solvents were of reagent grade and used without further purification. The ligand 5-(3-methyl-5-(pyridin-4-yl)-4*H*-1,2,4-triazol-4-yl) isophthalic acid (H_2**L**) was synthesized according to the method reported previously [17]. X-ray powder diffraction (PXRD) intensities were measured on a Rigaku D/max-IIIA diffractometer (Cu-*K*α, $\lambda = 1.54056$ Å). The single crystalline powder samples were prepared by crushing the crystals and scanned from 3° to 60° with a scanning speed of 0.02°/s. Thermogravimetric analysis (TGA) were performed on a NETZSCH TG 209 instrument with a heating rate of 10 °C/min in the N_2 atmosphere. Flourescence spectroscopy data were recorded on HORIBA Jobin Yvon HJY-FL3-221-TCSPC spectrophotometer.

2.2. Preparation of coordination polymers

2.2.1. Synthesis of $[Cu(HL)]_n \cdot nH_2O$

$CuCl_2 \cdot 2H_2O$ (0.1 mmol, 0.017 g), H_2**L** (0.2 mmol, 0.0648 g) and $Sm(NO_3)_3 \cdot 6H_2O$ (0.1 mmol, 0.0444 g) were dissolved in 15 mL water, reacted for 20 min under the 100 W of ultrasound, transferred to a 25 mL Teflon-lined pot, and the reaction mixture was heated within 2 h up to 140 °C. The temperature was kept on a constant level for 3 days, and then the autoclave was cooled rapidly to room temperature. Brown block crystals of **1** were collected with a yield of 78% (based on Cu). Anal. calcd for $C_{16}H_{13}N_4O_5Cu$: C, 47.47; H, 3.24; N, 13.84. Found: C, 47.52; H, 3.14; N, 13.90. IR data (KBr pellet, ν[cm^{-1}]): 3419.61, 2362.76, 2342.41, 2026.88, 1619.15, 1544.96, 1373.96, 1306.30, 1251.18, 1132.83, 879.04, 840.91, 623.85, 488.66.

2.3. Analysis of the residual carboxyl groups of compound *1*

Compound **1** was first immersed in rhodamine B (0.1 wt%) in sodium phosphate buffer (0.1 M, pH 8) for 5 min. After rinsing with DI water and drying in a stream of nitrogen, the rhodamine B stained compound **1** was imaged using fluorescent microscopy (excitation 540 ± 20 nm, emission 625 ± 20 nm) [14].

2.4. Protein adsorption analysis

Protein adsorption assay was performed following the method previously reported [14]. Protein solutions were freshly prepared by dissolving BSA or lysozyme in phosphate-buffered saline (PBS, 0.01 mol/L, pH 7.4) to give a final concentration of 20 mg/mL. Compound **1** (40 mg) was placed in 5 mL centrifugal tubes, to which 2 mL of the freshly prepared BSA or lysozyme was added. Adsorption was allowed to proceed at 37 °C for 2 h under gentle shaking. The suspension was then centrifuged and washed with PBS five times. The supernatant was collected together, filtered through a membrane of 0.45 μm pore diameter, and diluted to 500 mL with PBS buffer. The supernatant was analyzed by ultraviolet absorbance at 280 nm to determine the adsorption amount of protein. Three repetitions were performed for all samples. The adsorption of protein, P (mg/g), on compound **1** was calculated according the following formula:

$$P = \frac{[C_i]V_i - [C_r]V_r}{m}$$

where $[C_i]$ is the protein concentration in the initial solution ($mg_{Protein}/mL_{solution}$), $[C_r]$ is the residual concentration of protein in solution ($mg_{Protein}/mL_{solution}$), and m is the mass of compound **1** (g).

2.5. X-ray photoelectron spectroscopy (XPS) analysis

XPS spectra were recorded using a Kratos Axis Ultra DLD spectrometer employing a monochromated Al-*K*α X-ray source ($h\nu = 1486.6$ eV). The vacuum in the main chamber was kept above 3×10^{-6} Pa during XPS data acquisitions. General survey scans (binding energy range: 0–1200 eV; pass energy: 160 eV) and high-resolution spectra (pass energy: 40 eV) in the regions of N1*s* were

Table 1
Crystal data and structure refinements for compound 1.

Identification	Compd **1**
Empirical formula	$C_{16}H_{13}CuN_4O_5$
Formula weight	404.84
T (K)	293(2)
Crystal system	Monoclinic
Space group	$C2/c$
a (Å)	17.035(3)
b (Å)	10.172(2)
c (Å)	19.396(4)
α (°)	90
β (°)	113.62(3)
γ (°)	90
Z	8
ρ_{calc} (g cm^{-3})	1.747
μ (mm^{-1})	1.458
F(0 0 0)	1648
2θ scan range	4.58 to 50.02°
Reflections collected	12,530
R_{int}	0.1068
Independent reflections	2705
Parameters	240
Goodness-of-fit on F^2	1.093
R_1,wR_2[$I > 2\sigma(I)$]	0.0428, 0.0975
R_1,wR_2[all data]	0.0491, 0.1036

Table 2
Selected bond lengths [Å] and angles [°] for **1**

Selected bonds (Å) and angles (°)			
N(3)–Cu(1)#1	1.970(2)	N(2)–Cu(1)–N(3)#2	131.60(9)
Cu(1)–N(2)	1.965(2)	N(2)–Cu(1)–N(4)#3	113.23(9)
Cu(1)–N(3)#2	1.970(2)	N(3)#2–Cu(1)–N(4)#3	110.50(9)
Cu(1)–N(4)#3	2.068(2)	N(2)–Cu(1)–O(3)#4	90.87(9)
Cu(1)–O(3)#4	2.220(2)	N(3)#2–Cu(1)–O(3)#4	109.30(9)
N(4)–Cu(1)#3	2.068(2)	N(4)#3–Cu(1)–O(3)#4	89.60(8)
O(3)–Cu(1)#5	2.220(2)	N(2)–N(4)–Cu(1)#3	114.46(16)
		N(4)–N(2)–Cu(1)	122.61(17)

Symmetry transformations used to generate equivalent atoms: #1$x-1/2, y-1/2, z$; #2$x+1/2, y+1/2, z$; #3 $-x+3/2, -y+1/2, -z$; #4 $x, -y, z-1/2$; #5 $x, -y, z+1/2$.

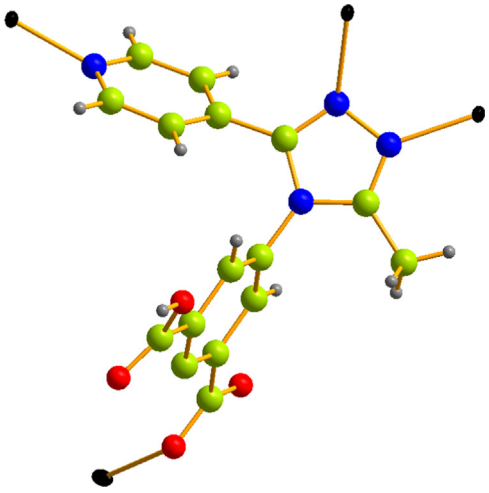

Scheme 1. Coordination Modes of the ligand HL^- in compound **1**.

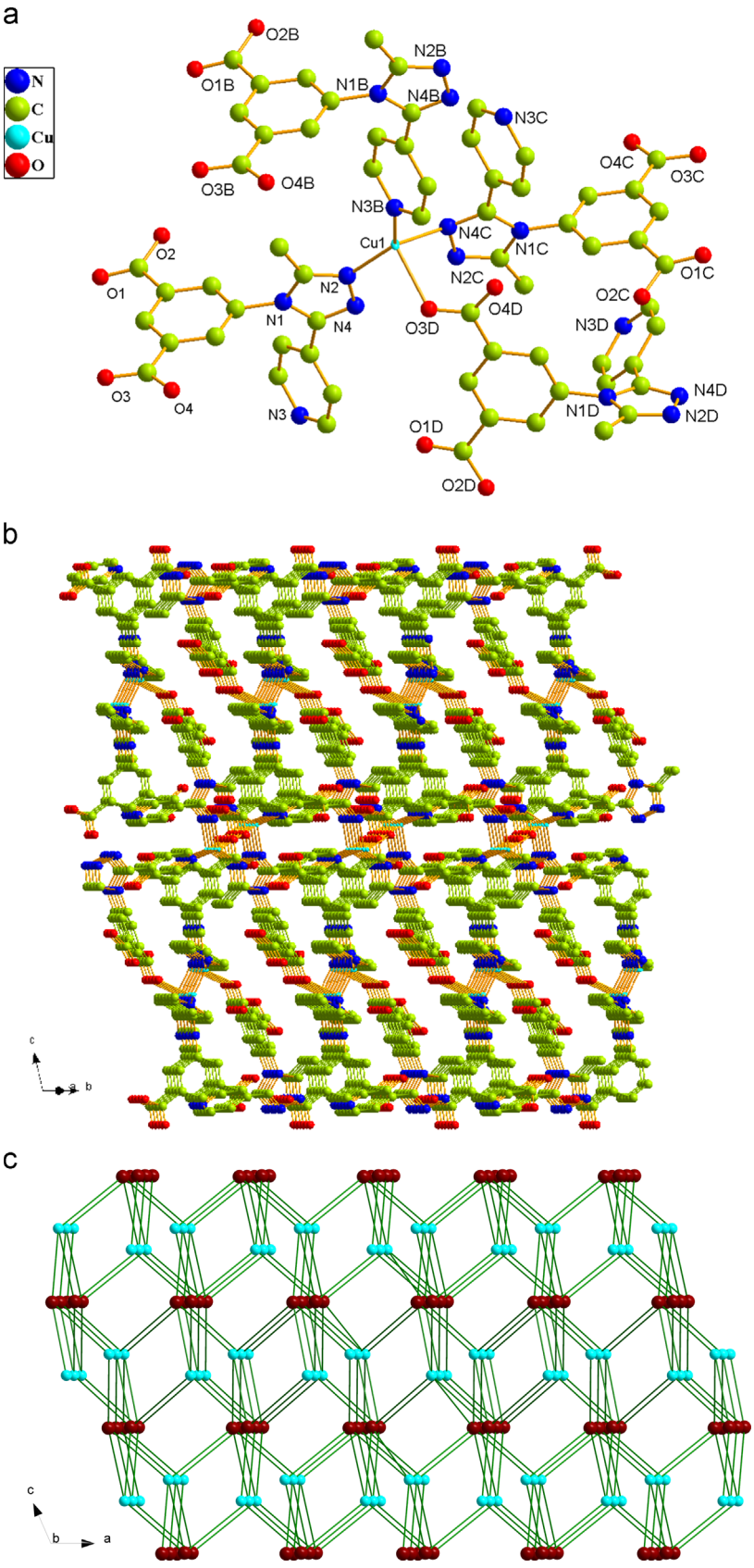

Fig. 1. (a) Coordination environment of the Cu^{I} ion. (b) 3D MOF of **1** running along the bc-plane. (c) The topology in **1** along the ac-plane (All hydrogen atoms are omitted for clarity).

recorded. Binding energies were referenced to the C1*s* binding energy at 284.60 eV.

2.6. X-ray crystallography

Diffraction data for compound **1** was collected with a Bruker SMART APEX CCD instrument with graphite monochromatic Mo*K*α radiation (λ=0.71073 Å). The data were collected at 293(2)K. The absorption corrections were made by multi-scan methods. The structure was solved by charge flipping methods with the program Olex2 and refined by full-matrix least-squares methods on all F2 data with Olex2. The crystallographic details are provided in Table 1, and selected bond lengths and angles for **1** are given in Table 2.

3. Results and discussion

3.1. Crystal structure

In compound **1**, the H**L**$^-$ ligand presents only one coordination mode (see Scheme 1: configuration μ4 for H**L**$^-$). In compound **1**, crystallizing in the monoclinic system, with the *C*2/*c* space group. As shown in Fig. 1a, the asymmetric unit of **1** consists of one crystallographically independent Cu^I ions, one H**L**$^-$ ligand, and one lattice water molecule. Cu1 is four-coordinated, four donors are one N2 atom near to methyl group of the triazole ring from one H**L**$^-$ ligand, one N4C atom near to pyridyl group of the triazole ring from another H**L**$^-$ ligand, one N3B atom of the 4-pyridine ring from the third H**L**$^-$ ligand, and one O3D atom of the fourth H**L**$^-$ ligand. The Cu–N distances range between 1.965(2) and 2.068(2) Å, and the Cu–O bonds are 2.220(2) Å. Thus, Cu^I site has a tetrahedral geometry, which is indicated by the bond angles: N(2)–Cu(1)–N(3)*B*=131.60(9)°, N(2)–Cu(1)–N(4)*C*=113.23(9)°, N(3)B–Cu(1)–N(4)*C*=110.50(9)°, N(2)–Cu(1)–O(3)*D*=0.90.87(9)°. In Fig. 1b, a three-dimensional network structure could be formed by the H**L**$^-$ ligands and Cu^I ions along bc-plane. The remaining carboxyl groups could be seen from the 3D skeleton. The Cu^I centers could be viewed as 4-*c* nodes, and the H**L**$^-$ ligands could be viewed as linkers. An xfe-4-Fddd, (4^2.6.8^3) topology in **1** is created (Fig. 1c).

Compared to $^3_\infty$[Cu(Me-4py-trz-ia)] from Lässig et al. [18], a microporous MOF was formed by the Cu^{II} centers and Me-4py-trz-ia^{2-} ligands. While in compound **1** here, the H**L**$^-$ ligands and Cu^I ions connected to 3D sheet; on the other hand, residual carboxyl groups were formed in compound **1** here, and no big holes were found (a calculated porosity of about 1.1% according to PLATON). In compound **1**, the Cu^{II} centers presents two coordination modes [18], but in compound **1** here, the Cu^I centers presents only one coordination mode. So a 3D **pts** topology is generated in compound **1** [18]; while an xfe-4-Fddd, (4^2.6.8^3) topology was formed in compound **1** here.

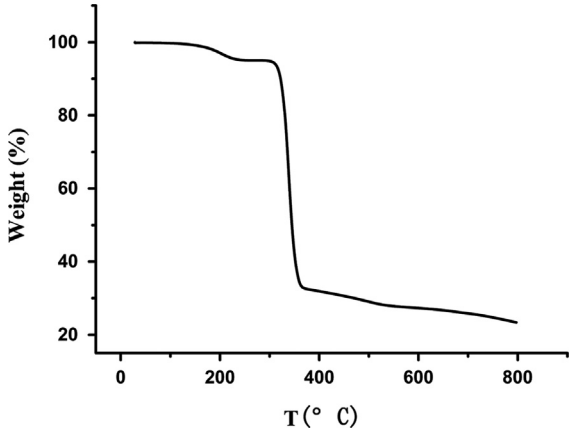

Fig. 2. TG curve of compound **1**.

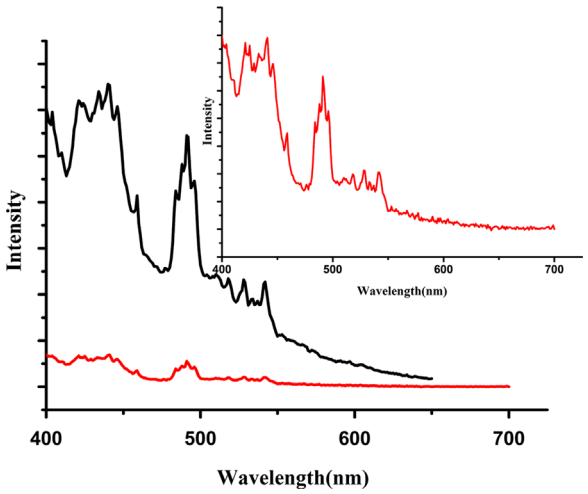

Fig. 3. Solid state emission spectra for compound **1** (red) and the H_2**L** ligand (black) at room temperature upon excitation at 370 nm (The insert image is the enlarged view of compound **1**). (For interpretation of the references to color in this figure legend, the reader is referred to the web version of this article.)

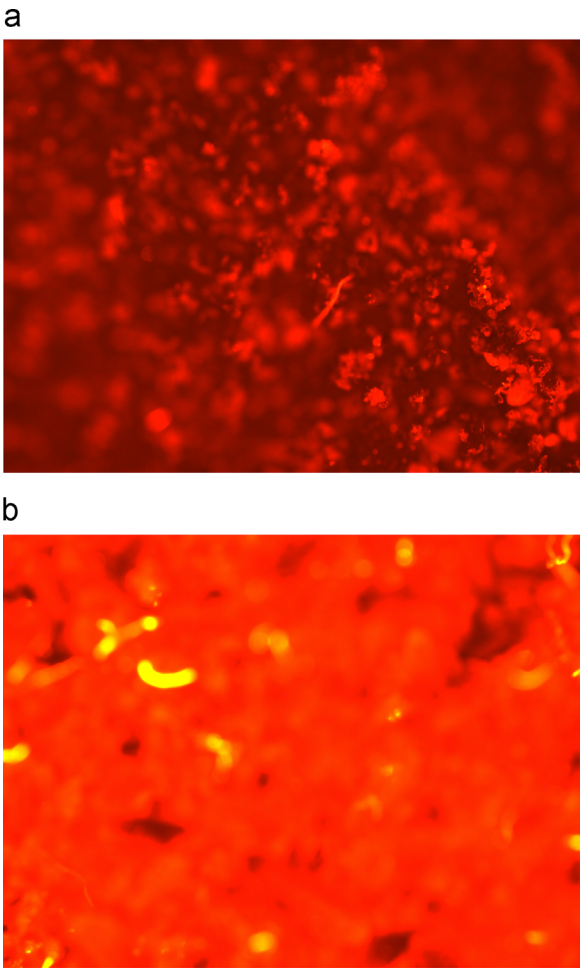

Fig. 4. (a) Fluorescence image of non-stained compound **1**. (b) Fluorescence image of the rhodamine B-stained compound **1** (both are magnified by four times).

3.2. Phase purity and thermal analysis

The purity of the powder samples was confirmed by PXRD. The PXRD pattern of compound **1** is illustrated in Fig. S1, which is in an agreement with the simulated one, confirming the phase purity of the as-synthesized product. The TGA were carried out on the crystalline samples in the N_2 atmosphere with a heating rate of 10 °C/min in the temperature range 25–800 °C.

The TG curve of compound **1** is illustrated in Fig. 2. The TG curve of compound **1** exhibits three main weight loss steps. The TG curve of compound **1** shows the first stage of weight loss from 131 °C to 238 °C (4.78% contrast to theoretical 4.45%), which is attributed to the release of the guest water molecule. The second stage of weight loss occurs from 298 °C to 368 °C (62.14%), which is attributed to the partial decomposition of the organic ligands. The third stage of weight loss occurs from 368 °C to 800 °C (9.75%), which is attributed to the partial decomposition of the organic ligands. The degradation of compound **1** is incomplete (17.67% base on the Cu_2O).

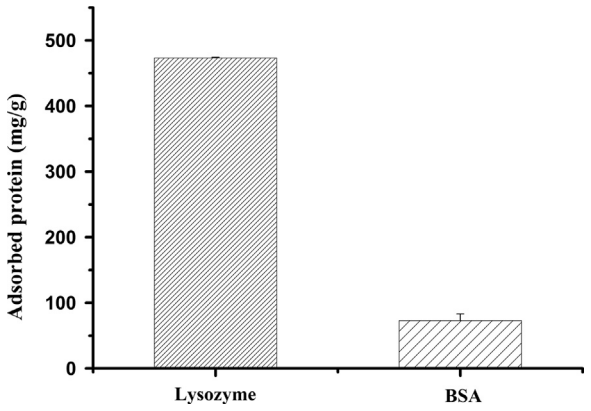

Fig. 5. Comparison of amount of lysozyme and BSA adsorption on the surface of compound **1**.

3.3. Emission properties

The fluorescence emission spectrophotometry of compound **1** and the ligand was studied in the solid state at room temperature (Fig. 3). The free ligand H_2**L** shows luminescence with the emission maximum at 441 nm and 492 nm, upon excitation at 370 nm. Compound **1** shows luminescence with the emission maximum at 441 nm and 491 nm, upon excitation at 370 nm, which is attributed to the internal transitions of the ligands. In contrast with the H_2**L** ligand, compound **1** shows decreased luminescence, which could be caused by the presence of free water molecules [19–22].

3.4. Analysis of the residual carboxyl groups of compound *1*

At pH 8, carboxyl groups of compound **1** could be changed to negatively-charged carboxyl anions. Rhodamine B has positively-charged amino groups and could adsorb to the negatively-charged carboxyl anions of compound **1** [23]. Stronger intensity of red fluorescence could be seen from the rhodamine B-stained compound **1**, in

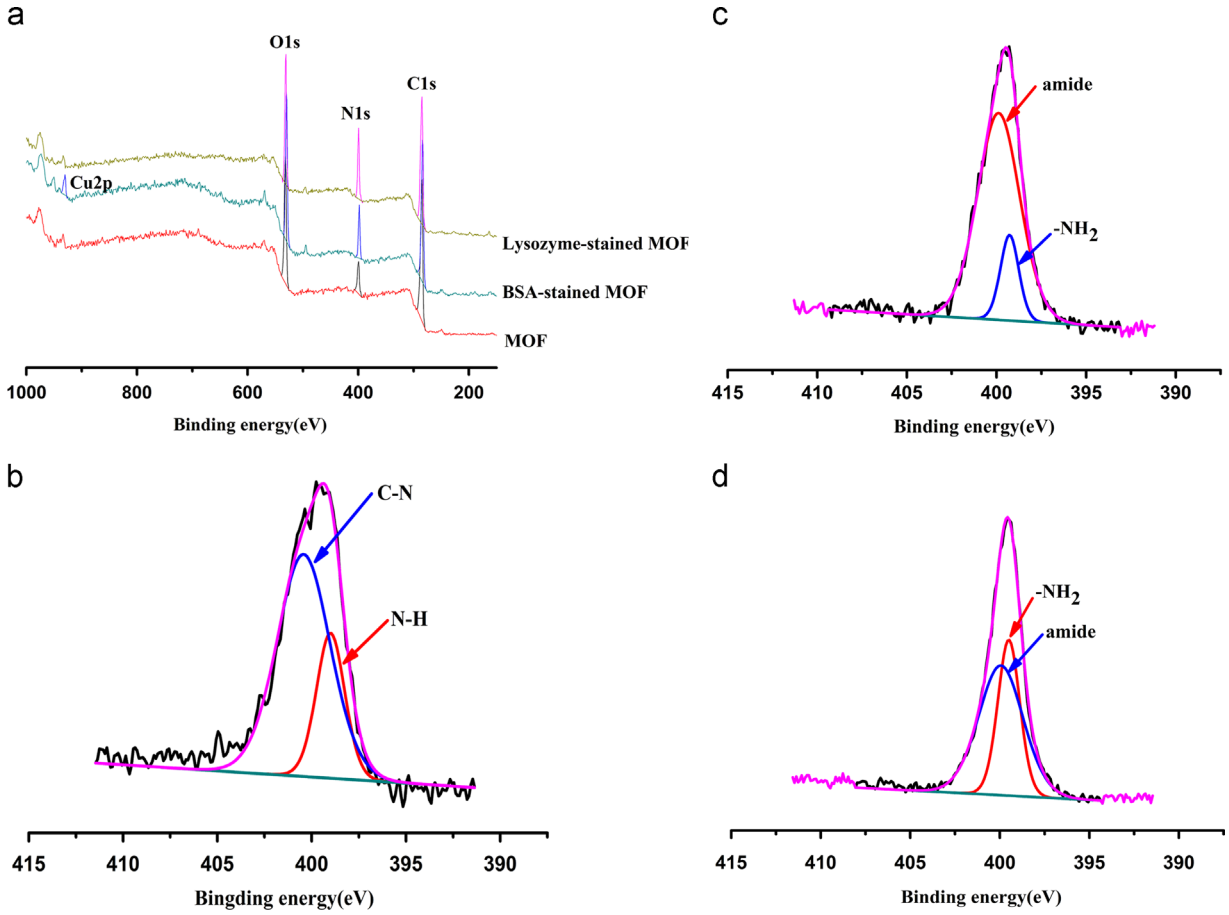

Fig. 6. (a) XPS wide scan spectra of compound **1** (non-dealed with PBS buffer), BSA-stained and lysozyme-stained compound **1**. (b) High-resolution XPS N1*s* spectra of compound **1** (non-dealed with PBS buffer). (c) High-resolution XPS N1*s* spectra of BSA-stained compound **1**. (d) High-resolution XPS N1*s* spectra of lysozyme-stained compound **1**.

contrast with non-stained compound **1**. The results (Fig. 4) exhibited that there were residual carboxyl groups on the surface of compound **1**, compared with the control (i.e., non-stained compound **1**).

3.5. Protein adsorption analysis

In physiological media, most proteins carry a net charge. There is a pH, at which a net charge is zero on the surface of each protein, that is, the isoelectric point of the protein (pI). Electrostatic interactions between proteins and charged surfaces, therefore, often play a major role in the adsorption behavior of proteins. Therefore, BSA and lysozyme were selected for protein adsorption assay in the current study. The amounts of protein adsorbed onto the surface of compound **1** are shown in Fig. 5a, which indicates that compound **1** tends to reduce BSA adsorption; but increase lysozyme adsorption. As mentioned above, compound **1** maintained residual carboxylic acid groups on the surface. At pH 7.4, the carboxylic acid of compound **1** was converted to a negatively-charged carboxylate ion. The pI value of BSA is 4.7. At pH 7.4, the net charge of BSA is negative. Therefore, BSA (pI 4.7), a carboxylic acid-rich protein was significantly less adsorbed onto the carboxylic acid-rich surface, possibly due to charge–charge repulsion [24]. On the other hand, lysozyme (pI 11), contains a large number of $-NH_2$ groups. Therefore, it is positively-charged at pH 7.4. Charge–charge attraction could be responsible for the increased adsorption of lysozyme. The results from this study seem to fit well with a previous report on the study of the charge interaction of protein and polyelectrolyte films [14].

3.6. X-ray photoelectron spectroscopy (XPS) analysis

Fig. 6a shows the low-resolution XPS survey spectra of these surfaces, all of which are semiquantitative. The XPS spectrum of compound **1** (non-dealed with PBS buffer) exhibited a ratio of 0.11 between the N1*s* and C1*s* photoemissions. A different N1*s*:C1*s* ratio of 0.16 was observed for BSA-stained compound **1**, 0.23 for lysozyme-stained compound **1**, indicating that protein adsorption changed the surface chemical compositions and more nitrogen was introduced. The low-resolution XPS survey spectrum of BSA-stained compound **1** has a peak of Cu 2*p* [25], which could be also showed in the pictures (Fig. S2, in supporting information). PBS buffer has changed the carboxylic acid to a negatively charged carboxylate ion. And part of compound **1** has been dissolved into PBS buffer and the color of solution has been changed to brown in non-stained compound **1** (dealed with PBS buffer) and BSA-stained compound **1**. But for lysozyme-stained compound **1**, no obvious dissolution happened and the solution was still transparent. This phenomenon could be better explained by more adsorption of lysozyme than that of BSA.

The high-resolution N1*s* XPS spectra (Fig. 6b) of compound **1** (non-dealed with PBS buffer) have peaks at 399.00 eV (C–N–Me) and 400.43 eV (–NH– groups, and perhaps, to a lesser extent, involvement in intermolecular hydrogen bonding interactions) [26,27]. High-resolution N1*s* XPS spectra (Fig. 6c) of BSA-stained compound **1** have peaks at 399.27 eV ($-NH_2$ groups) and 399.88 eV (amide groups from BSA) [28–32]. High-resolution N1*s* XPS spectra (Fig. 6d) of lysozyme-stained compound **1** have peaks at 399.50 eV ($-NH_2$ groups), and 399.94 eV (amide groups from lysozyme). After protein adsorption, the skeleton of compound **1** did not change, which could be seen from PXRD patterns (Fig. S3, in Supporting information).

4. Conclusions

In conclusion, a rare carboxyl-copper-organic framework, $[Cu(HL)]_n \cdot nH_2O$ (**1**) has been hydrothermally synthesized. An xfe-4-Fddd, ($4^2.6.8^3$) topology in **1** is created. Compound **1** shows decreased luminescence, in contrast with the H_2**L** ligand, which could be caused by the presence of free water molecules. There were residual carboxyl groups on the surface of compound **1**. BSA was significantly less adsorbed onto the carboxylic acid-rich surface; charge–charge attraction could be responsible for the increased adsorption of lysozyme. XPS spectra were also investigated to verify the results.

Acknowledgment

This work was supported by the National Natural Science Foundation of China (nos. 21371103, 21071083 and 20771062).

Appendix A. Supporting information

CCDC 951567 for compound 1 contains the supplementary crystallographic data for this paper. These data can be obtained free of charge from the Cambridge Crystallographic Data Centre via www.ccdc.cam.ac.uk/data_request/cif.

Supplementary data associated with this article can be found in the online version at http://dx.doi.org/10.1016/j.jssc.2014.05.019.

References

[1] Cheng Wang, Teng Zhang, Wenbin Lin, Chem. Rev. 112 (2012) 1084–1104.
[2] Z.G. Guo, R. Cao, X. Wang, H.F. Li, W.B. Yuan, G.J. Wang, H.H. Wu, J. Li, J. Am. Chem. Soc. 131 (2009) 6894–6895.
[3] H.H. Wu, R.S. Reali, D.A. Smith, M.C. Trachtenberg, J. Li, Chem. Eur. J 16 (2010) 13951–13954.
[4] J.R. Li, J. Sculley, H.C. Zhou, Chem. Rev. 112 (2012) 869–932.
[5] H.H. Wu, Q.H. Gong, D.H. Olson, J. Li, Chem. Rev. 112 (2012) 836–868.
[6] A. Lan, K. Li, H. Wu, D.H. Olson, T.J. Emge, W. Ki, M.C. Hong, J. Li, Angew. Chem. Int. Ed. 48 (2009) 2334–2338.
[7] R. Custelcean, M.G. Gorbunova, J. Am. Chem. Soc. 127 (2005) 16362–16363.
[8] J.S. Seo, D. Whang, H. Lee, S.I. Jun, J. Oh, Y.J. Jeon, K. Kim, Nature 404 (2000) 982–986.
[9] T. Gadzikwa, O.K. Farha, K.L. Mulfort, J.T. Hupp, S.T. Nguyen, Chem. Commun. (2009) 3720–3722.
[10] M.J. Ingleson, J.P. Barrio, J.B. Guilbaud, Y.Z. Khimyak, M.J. Rosseinsky, Chem. Commun. (2008) 2680–2682.
[11] E.I. Basaldella, J.C. Tara, G.A. Armenta, M.E. Patiño Iglesias, J. Porous Mater. 14 (2007) 273–278.
[12] S. Uchida, R. Kawamoto, H. Tagami, Y. Nakagawa, N. Mizuno, J. Am. Chem. Soc. 130 (2008) 12370–12376.
[13] J.P. Zhang, S. Kitagawa, J. Am. Chem. Soc. 130 (2008) 907–917.
[14] L.Y. Yang, L. Li, Q. Tu, L. Ren, Y.R. Zhang, X.Q. Wang, Z.Y. Zhang, W.M. Liu, L.L. Xin, J.Y. Wang, Anal. Chem. 82 (2010) 6430–6439.
[15] A. Vinu, K.Z. Hossian, P. Srinivasu, M. Miyahara, S. Anandan, N. Gokulakrishnan, T. Mori, K. Ariga, V.V. Balasubramanian, J. Mater. Chem. 17 (2007) 1819–1825.
[16] J.W. Shim, S.J. Park, S.K. Ryu, Carbon 39 (2001) 1635–1642.
[17] D. Lässig, J. Lincke, H. Krautscheid, Tetrahedron Lett. 51 (2010) 653–656.
[18] D. Lässig, J. Lincke, J. Moellmer, C. Reichenbach, A. Moeller, R. Gläser, G. Kalies, K.A. Cychosz, M. Thommes, R. Staudt, H. Krautscheid, Angew. Chem. Int. Ed. 50 (2011) 10344–10348.
[19] J.J. Wang, C.S. Liu, T.L. Hu, Z. Chang, C.Y. Li, L.F. Yan, P.Q. Chen, X.H. Bu, Q. Wu, L.J. Zhao, Z. Wang, X.Z. Zhang, CrystEngComm 10 (2008) 681–692.
[20] D.X. Xue, W.X. Zhang, X.M. Chen, H.Z. Wang, Chem. Commun. (2008) 1551–1553.
[21] T. Sun, J.P. Ma, R.Q. Huang, Y.B. Dong, Acta Crystallogr., Sect. E: Struct. Rep. Online 62 (2006) o2751–o2752.
[22] L.Y. Yang, L.F. Zeng, W. Gu, J.L. Tian, S.Y. Liao, M. Zhang, X.H. Wei, L.L. Xin, X. Liu, Inorg. Chem. Commun. 29 (2013) 76–81.
[23] Y.L. Wang, M. Bachman, C.E. Sims, G.P. Li, N.L. Allbritton, Langmuir 22 (2006) 2719–2725.
[24] V. Tangpasuthadol, N. Pongchaisirikul, V.P. Hoven, Carbohydr. Res. 338 (2003) 937–942.
[25] M.D. Silva Pinto, C.A. Sierra-Avila, J.P. Hinestroza, Cellulose 19 (2012) 1771–1779.
[26] C.M. Whelan, F. Cecchet, R. Baxter, F. Zerbetto, G.J. Clarkson, D.A. Leigh, P. Rudolf, J. Phys. Chem. B 106 (2002) 8739–8746.
[27] O. Olivares, N.V. Likhanova, B. Go´mez, J. Navarrete, M.E. Llanos-Serrano, E. Arce, J.M. Hallen, Appl. Surf. Sci. 252 (2006) 2894–2909.
[28] I. Frateur, J. Lecoeur, S. Zanna, C.O.A. Olsson, D. Landolt, P. Marcus, Electrochim. Acta 52 (2007) 7660–7669.

[29] A. Ithurbide, I. Frateur, A. Galtayries, P. Marcus, Electrochim. Acta 53 (2007) 1336–1345.
[30] S. Premathilaka, M. Hyland, X. Chen, B. Bansal, Food Bioprod. Process. 84 (C4) (2006) 265–273.
[31] C.M. Pradier, D. Costa, C. Rubio, C. Compere, P. Marcus, Surf. Interface Anal. 34 (2002) 50–54.
[32] G. Iucci, G. Polzonetti, G. Infante, L. Rossi, Surf. Interface Anal. 36 (2004) 724–728.
[33] Y. Cui, Y. Yue, G. Qian, B. Chen, Chem. Rev. 112 (2012) 1126–1162.
[34] W. Zhang, R.G. Xiong, Chem. Rev. 112 (2012) 1163–1195.
[35] P. Horcajada, R. Gref, T. Baati, P.K. Allan, G. Maurin, P. Couvreur, G. Férey, R. E. Morris, C. Serre, Chem. Rev. 112 (2012) 1232–1268.
[36] S.E.H. Etaiw, S.A. Amer, M.M. El-Bendary, J. Inorg. Organomet. Polym. 21 (2011) 662–672.
[37] S.E.H. Etaiw, A.S. Elsherbiny, A.S. Badr El-din, Chin. J. Chem 29 (2011) 1401–1410.
[38] H.L. Jiang, T.A. Makala, H.C. Zhou, Coord. Chem. Rev. 257 (2013) 2232–2249.
[39] N. Stock, S. Biswas, Chem. Rev. 112 (2012) 933–969.